Conductivity Sensor for Agricultural Substrates

Diogo Fernandes de Castro Brandão de Almeida
diogo.de.almeida@tecnico.ulisboa.pt

Instituto Superior Técnico, Lisboa, Portugal

October 2021

Abstract

Over irrigation and over fertilization created the necessity to monitor agricultural soils salinity levels. Considering that the electrical conductivity (EC) is a practical index of the total concentration of ionized solutes in an soil sample, EC is the most used method to measure soil salinity levels. To that effect, the aim of this project is to develop an *in situs* soil electrical conductivity measurement system capable of performing unattended measurements for both hydroponics substrates and mineral soils.

Several *in situs* measurement methods were studied to understand the benefits and limitations of each. Ultimately, the developed sensor is based on a new approach to the frequency domain reflectometry method (FDR). This method was chosen due to the fact that it can be used to measure both the soil apparent electrical conductivity (EC_a) and the soil water content (θ), as both parameters are crucial to estimate soil salinity. This document details the work conducted to developed the FDR measurement system described above, as well as the tests necessary to evaluate the performance of the developed system.

The system was developed using a Digilent board FPGA board, combined with a ADC/DAC board and an external eletrical circuit. The FPGA was programmed to acquire multiple measurement samples at a specific frequency set by a PC. These samples are then used to determine the soil complex impedance. Furthermore, the methods to obtain the soil salinity from the soil complex impedance are also described in this document. The system was tested in multiple impedances to ensure it performed as expected.
Keywords: FDR sensor, Soil sensor, Hydroponics sensor, Soil electrical conductivity

1. Introduction

Nowadays, agricultural soils are experiencing a drop in crop yield, in most part due to the increasing levels of soil salinity. This increase was mainly caused by over-irrigation and over-fertilization. To address this issue, producers are implementing ever more clever technologies on their farms to provide tailored insights on how to grow crops more efficiently. As a result, in the last decade agriculture technologies have seen a tremendous growth fueled not only by technological breakthroughs but also by the necessity of accurate soil nutrient measurements.

Still, these systems have to be further improved to allow their widespread application. Since the electrical conductivity EC, is a practical index of the concentration of ionized solutes dissolved in an soil sample, EC sensors offer a reliable measurement system for soil salinity assessment.

This project focuses on the implementation of an *in situs* soil electrical conductivity measurement system, mainly for nutrient management purposes and soil salinity appraisal. The system's working principle is based on frequency domain reflectometry (FDR) within a range of frequencies. This FDR method was tested on multiple soils using an impedance analyzer.

After ensuring that the FDR method performed as expected, a measurement system was developed using an FPGA board. The chosen board was a Nexys 4 FPGA board from Digilent, which incorporates an Artix 7 FPGA. The Nexys 4 board, combined with a ADC/DAC board and an external eletrical circuit, is used to measure complex impedances.

The FPGA's firmware was developed to acquire multiple measurement samples at a given frequency controlled by a PC, up to 10 MHz. The PC is also used to manage the FPGA and to process the sample's data, from which the complex soil impedance is calculated. The soil salinity can then be estimated using the complex soil impedance determined. The system was tested in impedances with know characteristics to ensure it functioned as expected.

2. State of the Art

Electrical conductivity (EC), denoted σ, is the ability of a certain material to conduct electrical cur-

rent. It is measured in siemens per meter (S/m) and it is usually estimated using the following expression

$$\sigma = \frac{l}{A} \cdot G \tag{1}$$

where l is the length of the material (m), A its the contact area of the electrodes (m^2) and G is the conductance (S). Since σ is the reciprocal of the electrical resistivity (ρ), it can be estimated using

$$\sigma = \frac{1}{\rho} \tag{2}$$

where $R = \frac{1}{G}$ is the electrical resistance (Ω).

Soil electrical conductivity assessments, were usually conducted through laboratory measurements of the electrical conductivity of the saturated soil paste extract (EC_e), since electrical conductivity is the most reliable indicator of the total dissolved ionic material in an aqueous sample [9].

However, the measurement of soil EC using EC_e, is not practical, being a very expensive method, since it requires the extraction of samples and posterior laboratory measurements. As a result, EC measurements are now being conducted using the apparent soil electrical conductivity (EC_a).

The assessment of soil salinity through the measurement of EC can be done using various measurement methods. The most used can be classified into electrical resistivity (ER), electromagnetic induction (EMI) and reflectometry, which is divided into time domain reflectometry (TDR) or frequency domain reflectometry (FDR). Nowadays, almost all monitoring applications use either TDR or FDR, since these methods can measure multiple soil properties besides EC such as the soil water content (θ). However, ER methods are still being used due to their simplicity.

2.1. Frequency Domain Reflectometry (FDR)

Frequency domain reflectometry, FDR, is a reflectometry method based on the electrical resonance of RLC circuits. A typical FDR circuit is presented in Figure 1.

The circuit comprises, amongst other elements, a lossy capacitor formed by two electrodes inserted in the soil as described in Figure 2. The lossy capacitor is modelled as a resistance (R_{soil}) and a capacitor (C_{soil}), the capacitance is given by

$$C_{soil} = g\varepsilon \tag{3}$$

where g is the capacitor design factor and ε is the soil dielectric permittivity. ε is a physical quantity that describes the response of the soil to an applied electric field, it is a complex number ($\varepsilon = \varepsilon' - j\varepsilon''$) [8].

The real part of ε, ε' represents the stored energy being mainly affected by the soil water content θ [3]. The imaginary part of ε, ε" represents the induced current energy loss and is mainly affected by the EC_a [11]. Therefore, by measuring ε, it is possible to estimate both EC_a and θ.

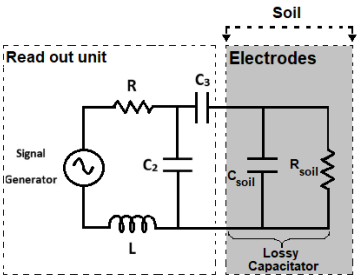

Figure 1: Typical circuit of a FDR sensor based on resonance frequency. Adapted from [11].

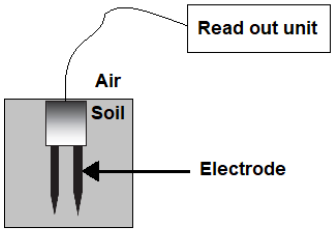

Figure 2: Single probe sensor.

The soil EC_a and ε can be estimated by measuring the complex impedance of the soil (Z_s) located between two electrodes. The complex impedance of the soil is represented as

$$Z_s = R + jX \tag{4}$$

The soil resistance (R) is influenced by the both soil salinity and θ, while the soil reactance (X) is mainly dependent on θ [5].

At frequencies between DC and 1 MHz the resistive component is much more significant than the reactive component as a result at these frequencies the measurement is more sensitive to soil salinity [5]. At higher frequencies, above 100 MHZ reactive component is much larger than the resistive component [5]. To take advantage of this fact, two different approaches can be employed, one estimates Z_s using different frequencies, below 1 MHz and around 100 MHz, to estimate R and X respectively. The other, estimates both R and X at the same frequency, usually around 10 MHz. From the values of R and X at these frequencies, R_{Soil} and C_{Soil} can be estimated.

Considering that the soil impedance is a complex value, to define it, both the module and phase are

necessary. The standard procedure to estimate Z_s involves applying a sinusoidal signal at a specific frequency value to the electrodes inserted in the soil. Afterwards, the amplitude and phase shift are measured through an analog-to-digital converter and signal processing algorithms [10]. Alternatively, the real and imaginary part of the current can be determined.

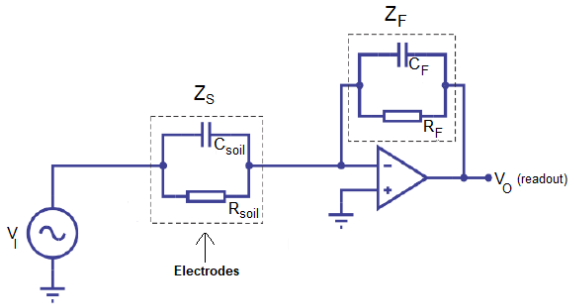

Figure 3: Auto-balancing bridge circuit. Adapted from [10].

The technique proposed in [10], auto-balancing bridge, estimates Z_s by conducting measurements at two different frequencies. The technique's circuit is illustrated in Figure 3. Here V_I represents the input voltage, Z_s is the unknown impedance, Z_f is the impedance feedback circuit and V_O is the measured output voltage,

The relation between V_O and V_I is

$$\frac{\mathrm{V}_O}{\mathrm{V}_I} = -\frac{\mathrm{Z}_S}{\mathrm{Z}_F} = -\frac{\mathrm{G}_S}{\mathrm{G}_F} = \frac{j\omega \mathrm{C}_{Soil} + 1/\ \mathrm{R}_{Soil}}{1/\ \mathrm{R}_f + j\omega \mathrm{C}_f}. \quad (5)$$

The system working principle is based on the fact that when $f \to 0$

$$\frac{\mathrm{V}_O}{\mathrm{V}_I} \approx \frac{1/\mathrm{R}_{Soil}}{1/\ \mathrm{R}_f + j\omega \mathrm{C}_f} \quad (6)$$

so R_{Soil} can be determined. On the other hand, when $f \to \infty$

$$\frac{\mathrm{V}_O}{\mathrm{V}_I} \approx \frac{j\omega \mathrm{C}_{soil}}{1/\ \mathrm{R}_f + j\omega \mathrm{C}_f} \quad (7)$$

so C_{Soil} can be obtained.

Finally R_{Soil} and C_{Soil} can be estimated as

$$\mathrm{Z}_s = \underbrace{\frac{\mathrm{R}_{soil}}{1 + (\omega\, \mathrm{C}_{soil}\mathrm{R}_{soil})^2}}_{\mathrm{R}} + \underbrace{j\frac{-\omega\, \mathrm{C}_{soil}{\mathrm{R}_{soil}}^2}{1 + (\omega\, \mathrm{C}_{soil}\mathrm{R}_{soil})^2}}_{\mathrm{X}}. \quad (8)$$

Then, R_{Soil} is related to EC_a through (1) and R_{Soil} is related to ε using (3). The method proposed in this project is based on the method described above however, instead of measuring Z_s for a specific frequency value, it will measure Z_s over a particular frequency range.

Considering the high operating frequencies of TDR sensors, this systems are extremely complex to develop, inflating its price. As a result, FDR sensors provide a better alternative seeing that in terms of accuracy both methods are similar and FDR systems are much simpler to design.

3. The assessment of soil salinity

Soil EC_a is affected by a great variety of soil properties, as a consequence, trying to estimate particular soil properties through EC_a is not an easy task. Mathematical methods to estimate particular soil properties are complicated since they have to take into account other soil properties that may affect EC_a measurements. In order to measure soil salinity through EC_a, it is necessary to choose the right method to relate EC_a with EC_e.

The first option are deterministic models, multiple parameters must be known to estimate EC_e. This creates a problem since the parameters cannot all be measured with the same sensor and many of them are site specific. Furthermore, the calibration equations usually cannot be used in multiple locations [2]. However, this approach is preferred when significant changes in soil properties occur between the measured soils [1].

On the other hand, statistical modelling techniques can be used as an alternative to deterministic methods. With statistical methods, the model parameters are estimated based on calibrations. These calibrations are done by measuring multiple soil salinity values and then using regression techniques alongside other known soil properties to predict unknown EC_e values. An EC_e average can then be estimated using [11]

$$\mathrm{EC}_e = \mathrm{EC}_a \cdot P \quad (9)$$

where P is the calibration obtained from the regression methods. The two most used stochastic methods are co-kriging regression and multiple linear regression.

Contrary to the stochastic methods mentioned above, deterministic methods are static. Most deterministic methods take advantage of the relation between, θ, EC_a and EC_e. The EC_a can be modelled as a function of soil properties according to [6]

$$\mathrm{EC}_a = \theta(a\theta + b)\sigma_p + (a\theta + b)B\rho_b CEC \quad (10)$$

where $(a\theta + b)$ is the transmission coefficient, a and b are fitting parameters dependent on soil texture and structure, B is the equivalent conductance of the counterions on the soil exchange complex (S m^2/mmolC), ρ_b is the soil bulk density (kg/m^3) and CEC, given in mmolC/kg, is dependent on soil

texture, clay mineralogy, and organic matter content. Due to θ's space and time variability, the model represented in (10) can only be used in sensors that measure EC_a and θ simultaneously. Assuming that this type of sensors are used, the Malicki method [7], determines EC_p using the empirical linear relation between EC_a and ε as

$$\mathrm{EC}_p = \frac{X_S}{m} = \frac{\mathrm{EC}_a - \sigma_s}{m(\varepsilon - \varepsilon_{ss})} \tag{11}$$

where m is the slope of X_S in relation to other soil characteristics, σ_s is the particle surface EC and ε_{ss} is the soil solids dielectric permittivity. Both these values need to be either estimated or measured [11]. Reference [12] provides regression equations for σ_s and ε_{ss}, dependent on clay content and specific surface. Optimally, these equations should be determined, through measurements, for each soil type. The process is detailed in [12]. For soils with very low values of EC_a, the accuracy of σ_s and ε_{ss} is critical.

The Hilhorst model [4] was developed based on (11). The relationship is represented by

$$\mathrm{EC}_p = \frac{\varepsilon_p}{\varepsilon - \varepsilon_0}\mathrm{EC}_a \tag{12}$$

where ε_p is the dimensionless dielectric constant of soil water, which is considered to be (ε_p = 80) and ε_0 is the value of ε when EC_a = 0, a constant. In [4] was found that it's value ranges between 1.9 and 7.6.

Stochastic methods are preffered for soils with similar characteristics. Seeing that deterministic methods include multiple soil specific parameters, this approach is preferred when significant differences exist between soils. However, since many of this parameters are difficult to obtain, most deterministic methods are unpractical for *in situs* measurements.

Statistical methods estimate the model parameters based on calibrations. The most used of these methods are the co-kriging regression and multiple linear regression. The methods present similarities in their accuracy, however, MLR is more advantegeous since number of samples required is inferior.

Considering the determistic methods studied, the Hilhorst [4] is the most robust. Nevertheless, the literature is not consensual regarding its efficacy. For this method to be used in the developed system, its accuracy must be studied for the target soils.

4. Measurement System.

The soil impedance measurement system was developed around a Field Programmable Gate Array (FPGA). The system was designed as represented in Figure 4.

On the developed system, the PC is responsible for managing the measurements, controlling the FPGA, through the USB port, and setting each measurement's signal frequency. Additionally, it also processes all of the measurement's data and performs all the necessary calculations to determine Z_s, used to estimate EC_a and θ.

The FPGA handles the core functions of the measurement system, which can be divided into two different parts. The first, focuses on generating a sine wave to excite Z_s, the signal is converted on the DAC connected to the FPGA. The second FPGA function, relates to the ADC. On this part, the FPGA is responsible for receiving the measurement samples from the ADC and storing them in the memory before being sent to the PC to be processed.

The ADC/DAC board converts the sine samples generated by the FPGA, from digital to analog. It then converts the samples back form the measurement circuit, from analog and digital.

Finally, the measurement circuit, comprises all the additional components necessary to measure Z_s.

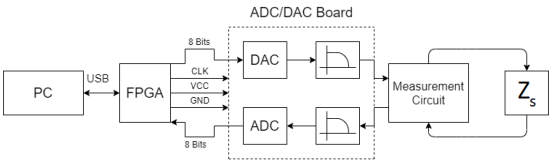

Figure 4: Schematic of the impedance measurement system developed.

5. PFGA

The FPGA is the main component of the impedance measurement system developed in this work. The board used is an Digilent Nexys 4 board which incorporates an Artix-7 FPGA. Also incorporated on the board, are a 4,860 Kbits BRAM, a 16Mbyte CellularRAM and a USB-UART Bridge.

The FPGA's implemented functionalities can be split into signal generation and measurement acquisition, as shown in Figure 5.

As presented in Figure 5, a MicroBlaze soft processor is used to control the blocks of the FPGA. The MicroBlaze communicates with a PC, which sets a given measurement's signal frequency and receives the measurement's samples. The PC and the FPGA communicate through the USB-UART Bridge.

The signal generation main block is the direct digital synthesizer (DDS), which receives a frequency value from the MicroBlaze and generates a output sine wave with the received frequency.

In Figure 5 it is possible to see that ,the measurement's acquisition part is more complex. In order

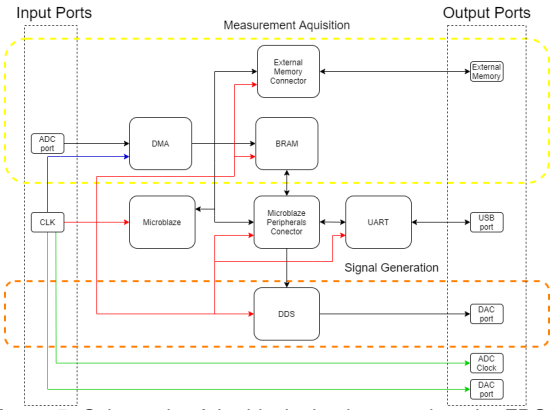

Figure 5: Schematic of the blocks implemented on the FPGA.

to store the highest number of samples as possible, the 16 MByte cellular RAM is used. Since the ADC receives the signal at a 30 MHz sample rate, it's not possible to write the values directly to the external memory.

A Direct Memory Access block (DMA) is connected to the ADC port and writes the samples directly to the BRAM. When the BRAM is full, the DMA stops writing data to the BRAM. At this point, an interruption is sent to the MicroBlaze which transfers this block of samples from the BRAM to the cellular memory. When the data transfer finishes, the MicroBlaze reactives the DMA which writes another block of data to the BRAM. This process is done until he cellular memory is full.

5.1. Firmware

The MicroBlaze is a soft microprocessor, which can be programmed using C language. The C code developed, is used to configure and control the FPGA blocks and to communicate with the PC. Figure 6, provides a simple overview of the MicroBlaze's main functioning.

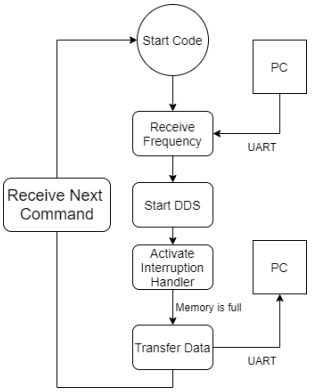

Figure 6: Schematic of the MicroBlaze's code flow.

As can be observed in Figure 6 the first step of the code is to receive the frequency value from the PC. Figure 7 shows how this function is implemented.

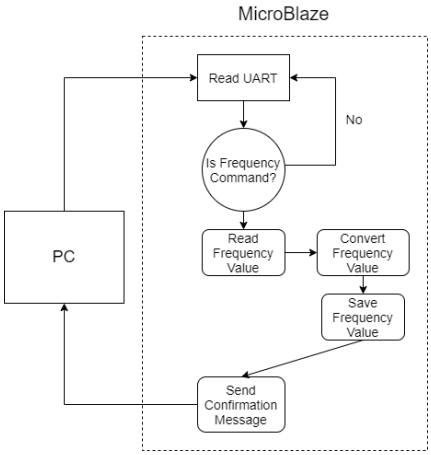

Figure 7: Flow of the function developed to read frequency values sent from the PC.

When the system initiates, the MicroBlaze starts a continuous loop, waiting to receive the frequency command, sent by the PC, informing the MicroBlaze that the next value to be received is the frequency value. The value is then saved and the confirmation message is sent to the PC. This message informs the PC that the frequency value was well read. The PC then, waits for the microblaze to sendd the measurement values.

The next step is to set the phase increment value on the DDS, which then starts to generate a sine wave with the frequency correspondent to the phase increment set.

After the DDS starts to run, the MicroBlaze interruption handler is activated. This interruption is controlled by the DMA, when the BRAM is full, the MicroBlaze interruption routine is called. The routine functions as shown in Figure 8.

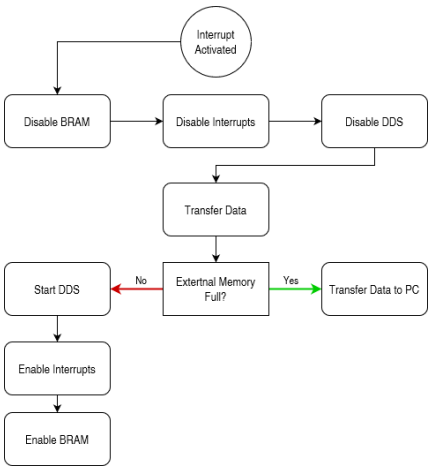

Figure 8: MicroBlaze's interruption routine.

When an interruption is called, the routine immediately disables the BRAM (through the DMA "ps_en" port). Afterwards, the interruption handler is disabled to make sure other interruptions can't be called while the routine is running. The DDS is also disabled since the output values aren't being read by the DMA.The MicroBlaze then transfers the data from the BRAM to the cellular memory.

The function that transfers the data from the BRAM to the external memory, receives the previous external memory address as an argument. Thereby, the new data can be written on the next address making sure that no address is missed and that the full size of the cellular memory is used. The function reads the first address from the BRAM and writes the data to the cellular memory, then the BRAM's address is incremented by 4 and the external memory address is incremented by 1. This loop continues until the all data on the BRAM is transferred. At this stage, the function returns the last external memory address where the data was written.

When the data transfer is completed, if the cellular memory is not full, the MicroBlaze waits for another interruption to run the same process. For this to happen, the DDS is reset (with a phase equal to 0) and restarted at the same frequency as before. The interruption handler is then enabled and the BRAM starts to read new measurement's values.

On the contrary, if the external memory is full, the function to transfer the data from the BRAM to the external memory is run. The behaviour of this function is shown in Figure 9.

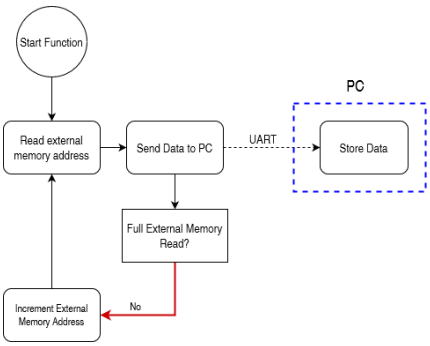

Figure 9: Function implemented to transfer the data from the external memory to the PC.

6. PC

As described above, the PC is responsible for controlling the FPGA, processing the measurement's samples and making all the calculations to determine Z_s. These processes are implemented on the PC using Python 3.10. The PC communicates with the FPGA through a USB port using a specific Python library (serial.py) at a rate of 230400 bits/s. Figure 10 describes in further detail the functions performed on the PC.

The frequency to be used on a specific measurement. is set on the PC. This frequency value is used to calculate the phase increment value that is sent to the FPGA. After receiving the phase increment value, the FPGA's DDS generates a sine at the defined frequency (sent to the DAC) and stores the measurement samples (received from the ADC).

The samples are then sent to the PC. At this stage, the PC processes the samples, removing unnecessary samples and converting the values from bits to Volts. With the samples converted, all the calculations are performed to determine the Z_s value, which is then used to determine EC_a and θ. The PC could then be configured to conduct multiple measurements at different frequencies (i.e swepping a frequency range).

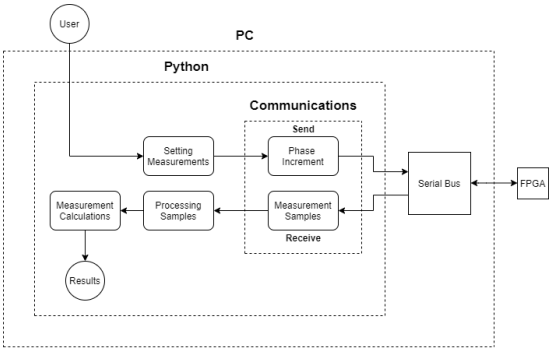

Figure 10: Schematic of the functions conducted by the PC.

6.1. Setting the Measurements

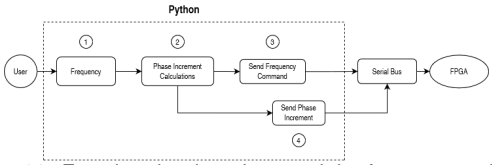

Figure 11: Function developed to send the frequency value to the MicroBlaze.

Figure 11 describes the steps performed by the PC to set the frequency for a specific measurement. The first step of the process, starts with the user setting the desired frequency, 1. The phase increment is calculated 2 using (13)

$$\Delta\theta = \frac{f_{out} \times 2^{32}}{120 \times 10^6} \tag{13}$$

There are multiple flows of information running between the FPGA and the PC. As a result, before sending the phase increment value to the FPGA 4 a command, 3 is sent. This command, informs

the FPGA that the next value to be received is the phase increment value. After the phase increment value is received, the FPGA sends and "OKAY" message to the PC.

Once these processes are complete, the FPGA receives the phase increment and the PC starts an active listing routine, waiting for the FPGA to send the measurement samples.

6.2. Processing Samples

The processes described in this sub-section represent 4 from Figure 10. The samples are received as a list of size K (dependent on the number of blocks read) and with the values ranging from 0 - 255. Upon receiving a given measurement's samples, the PC processes them.

The samples are processed in two main steps: 1 - removing the transition samples and 2 - converting the sample values to voltage, as described in Figure 12.

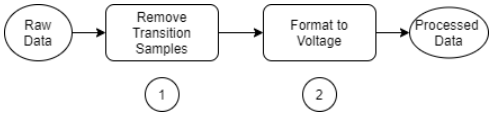

Figure 12: Steps to process the data received from the MicroBlaze.

As explained on Section 5 after each sample block is read, the DDS is reset. As a result, at the beginning of each block in the memory, some samples correspond to the transition stage of the DDS. These samples must be removed since they aren't relevant to the measurement of Z_s and could skew the obtained values. The first step 1 of the sample processing, is to remove this "transition samples", it was determined that, per block, the last 247 samples correspond to transition samples. Therefore, from the 8190 samples in a block (see Section 5), the last 247 are removed.

The values of the samples received range between 0 and 255 as a result, they must be converted into voltage values using,

$$V_{i,v} = -V_0 + V_{i,bits} \times \frac{V_0}{128} \qquad V_{i,bits} < 128 \quad (14)$$

$$V_{i,v} = (V_{i,bits} - 128) \times \frac{V_0}{128} \qquad V_{i,bits} \geq 128 \quad (15)$$

Once the samples are processed, 1 and 2, the values can be used to determine Z_s.

6.3. Measurement Calculations

The calculations described in this sub-section represent 5 from Figure 10. Represented on Figure 13 is the circuit used to measure Z_s. The circuit used an Analog Devices AD8066 operational amplifier. The AD8066 has multiple perfomance limitations, critical in the scope of this project. A worldwide scarcity of eletronic components made it impossible to find a more suitable amplifier.

In Figure 13, V_0 is the output value generated by the FPGA and V_i is the measurement value read by the FPGA.

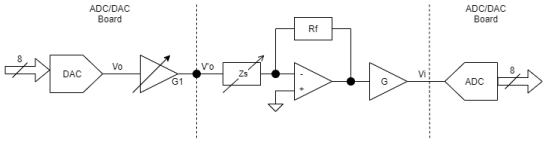

Figure 13: Schematic of the circuit used to measure Z_s.

The behaviour of the measurement circuit (Figure 13) can be represented by (16) and (17):

$$V_i = V_o G_1 \left(-\frac{R_f}{Z_s}\right) G; \qquad (16)$$

where V_O is the the output voltage of the DAC, G_1 is a potentiometer that controls the amplitude of V_O, Z_s is the (soil) impedance to be measured, R_f is the reference resistor used, G is the gain of the amplifier, V_i is the input voltage into the ADC.

For a specific frequency, f_0 generated on the DDS, its discrete Fourier transform (DFT) is

$$V_i(f_o) = \sum_{n=0}^{N-1} V_i(n) e^{-j2\pi \frac{f_o}{f_s} n} \qquad (17)$$

where $V_i(f_0)$ is the input voltage into the ADC for a given frequency, $V_i(n)$ is the input voltage of a given sample, f_0 is the sine frequency for a given frequency, f_s is the sample frequency (30 MHz) and N is the number samples.

Since the samples are divided in multiple, M, measurement blocks, an average of the $V_i(f_0)$ must be obtained,

$$\overline{V_i(f_o)} = \frac{1}{M} \sum_{m=0}^{M-1} V_{i,m}(f_0) \qquad (18)$$

Seeing that the behaviour of the circuit is dependent on the frequency, a calibration process must be conducted. This procedure is performed using a calibration impedance (R_{cal}), with known impedance values, in place of Z_S. The value of R_{cal} must be chosen in combination with the amplitude of V'_o, controlled by G, R_f and G_1.

Considering, Z_s = R_{cal} equations (16) through (18) are used to obtain V_{ical}.

With the values of V_i and V_{ical}, already calculated, the value of Z_s can be determined

$$\frac{V_i}{V_{ical}} = \frac{V_o G_1 \left(-\frac{R_f}{Z_s}\right) G;}{V_o G_1 \left(-\frac{R_f}{R_{cal}}\right) G;} = \frac{R_{cal}}{Z_s} \tag{19}$$

Finally,

$$Z_s(f_0) = R_{cal} \times \frac{\overline{V_{ical}(f_0)}}{\overline{V_i(f_0)}} = X + jY \tag{20}$$

After $Z_s(f_0)$ is obtained, (21) and (22) are used to determine the module and phase of Z_s, respectively,

$$|Z_s(f_0)| = \sqrt{X^2 + Y^2} \tag{21}$$

$$\sphericalangle Z_s(f_0) = (Y, X) \tag{22}$$

Considering that the complex value of Z_s is the necessary value to obtain R_{soil} and C_{soil}. These values, can then be applied to determine the values of EC_a and θ, ultimately used to estimate the soil salinity, EC_e.

7. Impedance Measurement

The setup used to test the measurement system developed is shown in figure 14. 1 - is the computer used to run the python code that controls the FPGA. 2 - is the Nexys 4 FPGA board used to develop the measurement system. 3 - is the DAC/ADC board connected to the FPGA through the PCB bridge. The two coaxial cables, input and output, are then connected to the measurement circuit - 4.

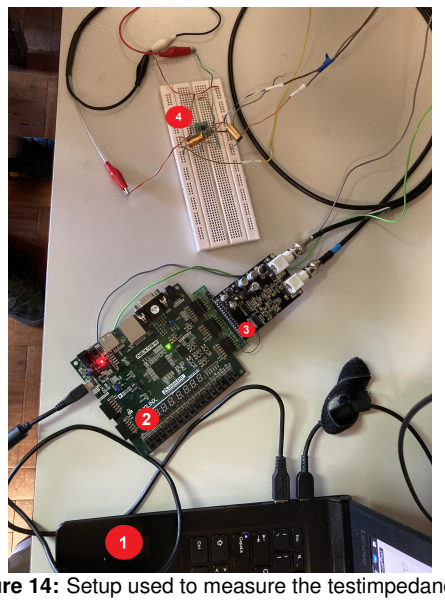

Figure 14: Setup used to measure the testimpedances.

Two different impedances were used Z_1 and Z_2. The measurement system combined with the circuit on figure 13 were used to perfom measurements on these impedances. Z_1 and Z_2 are represented as Z_s in figure 13.

Both the FPGA board and the ADC/DAC module contain filters on their circuit, as a result it is critical to understand if the filters characteristics affect the system's behaviour for different frequencies. Z_1, a 8.2 kΩ resistance, was for this purpose.

Z_2 is a test impedance, composed by a 8.2 kΩ resistance in series with a 68 pF capacitor. Unfortunatelly, the deadline for this project, made it unfeseable to perfom these tests on soil samples and other impedances.

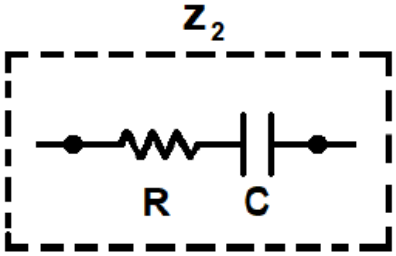

Figure 15: Setup used to measure the testimpedances.

As described earlier, for a given frequency, a calibration measurement was performed to determine V_{ical}, before each impdance measurement. This value is then used to obtain Z_s, using 20. Each of the impedances, Z_1 and Z_2, was measured for multiple frequencies between 10 kHz and 2 MHz. Ideally, the test should have be conducted with higher max frequency values, around 15 Mhz. However, the amplifier used AD8066, is not able to work properly beyond a 1 MHz frequency input. Due to a worldwide scarcity of eletronic components, it was not possible to source a more suitable operational amplifier.

The results obtained correlate with the theoreticall prediction considering the types of impedances used. For Z_f=R, the real part is similar to the theoritical value (8.2 kΩ). The Imaginary part, is equal to 0, since the impedance is only composed by a resistance. For the 2 MHz sample, the values deviate significantly from the theoretical value, as the amplifier does not work adequately beyond 1 MHz frequency inputs. The same occurs for Z_f=R+C.

Figure 16 represents the behaviour of Z_f=R for multiple frequencies. Two lines are represent, the measured value, red, and the theoretical value, blue. As can be observed, the measured value varies between 8201.79 Ω and 8192.87 Ω. Considering the deviations from the theoretical Z_f value (8.2 kΩ), it can be concluded that the measurement system precision, doesn't change significantly with the input signal frequency.

A comparison between the measured and

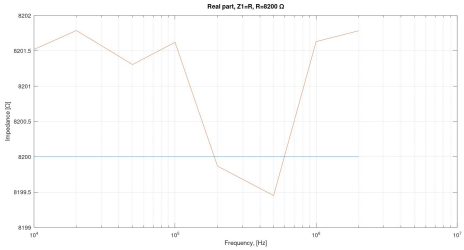

Figure 16: Real part of Z_f=R with R=8.2 kΩ. Comparison betweeen the measured and theoretical value, red and blue respectively.

therotical values of Z_f=R+C, red and blue respectively, was also conducted. This is depicted on Figures 17 and 18. For lower frequencies, 10 kHz, the real part of the measured value, is very different from the theoretical value. This can be caused by the filters on the FPGA board. In Figure 18, it can be seen that the imaginary part of Z_f=R+C, decreases with the frequency similar rate as the theoretical prediction.

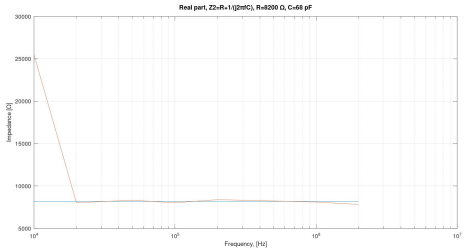

Figure 17: Real part of Z_f=R+C with R=8.2 kΩ and C=68 pF. Comparison betweeen the measured and theoretical value, red and blue respectively.

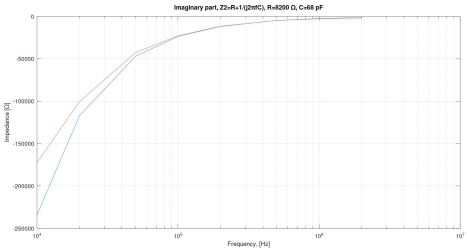

Figure 18: Imaginary part of Z_f=R+C with R=8.2 kΩ and C=68 pF. Comparison betweeen the measured and theoretical value, red and blue respectively.

Figures 19 and 20 show the absolute value and phase of Z_f=R+C. The absolute value, decreases with the frequency, as is expected for this circuit. The same happens with the phase which, in module, decreases with the frequency. In Figure 19 it is possible to observe that, at lower frequencies, there is a noticable difference between the theoretical and the measured value. This difference occurs, since the value of R_{cal} is low. Seeing that, $\frac{R_{cal}}{|Z_s|}$ is low, the signal on the ADC input is also low. The signal doesn't fill the full range of bits of the ADC, causing a bigger error in the reading.

A low ADC input, also justifies the gap between theoretical and measured values at lower frequencies 20. At higher frequencies, the gap between values is most likely caused by the amplifier's response at such frequencies.

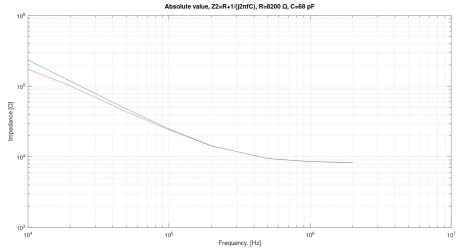

Figure 19: Absolute value of Z_f=R+C with R=8.2 kΩ and C=68 pF. Comparison betweeen the measured and theoretical value, red and blue respectively.

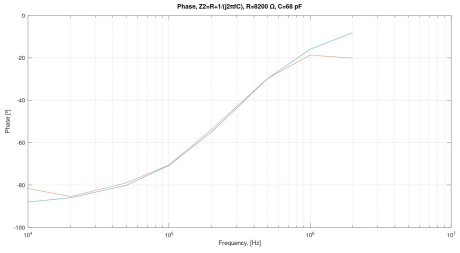

Figure 20: Phase of Z_f=R+C with R=8.2 kΩ and C=68 pF. Comparison betweeen the measured and theoretical value, red and blue respectively.

Overall, for both impedances, the values measured replicate the values predicted, at the studied frequencies. Although, with some error partircularly on the phase. More studies would have to be conducted, different impedance topologies and higher frequencies, to determine if the measurement system, behaves properly. Still, the electric circuit was very simple and the measurements were conducted with a calibration frequency of R_{cal} = 8200 Ω.

8. Conclusions

Electrical conductivity sensors are crucial to improve nutrient management in current agricultural productions. The goal of this project was to develop one of these sensors, an *in situs* electrical conductivity measurement system for soil salinity appraisal. An extensive analysis over the multiple methods to measure soil salinity, EC_e, *in situs* was performed. Based on this review, it was concluded

that FDR presents the most advantages for achieving the project's goal. This method is robust and practical, not only to develop, but also to use.

The system developed measures the soil complex impedance similarly to conventional FDR systems. However, the proposed method uses a different approach relative to the usual FDR techniques. The soil complex impedance is measured within a certain frequency range instead of only at a specific frequency value.

A measurement system was then developed to measure complex impedances using the aforementioned FDR method. For this, a Digilent Nexys 4 FPGA board in combination with an ADC/DAC module was used. The FPGA was programmed to aquire multiple samples at a frequency defined on the PC. This PC was used to control the FPGA and process a given measurement's data. The PC could then be programmed to performe a sequence of measurements, at different frequencies, thus measuring the complex impedance within a frequency range. The system was tested for specific impedances in order to ensure its correct funtioning. The complex impedance value obtained can then be used to determine the EC_a and θ, ultimately used to estimate EC_e.

The work developed on this project, presents a system capable of conducting complex impedance measurements at multiple frequencies. The system was implemented using the chosen *FDR method and can be used to perform electrical conductivity measurements for soil salinity appraisal.

References

[1] D. Corwin and S. Lesch. Application of soil electrical conductivity to precision agriculture. *Agronomy Journal*, 95, 05 2003.

[2] J. Doolittle and E. Brevik. The use of electromagnetic induction techniques in soil studies. *Geoderma*, s 223–225:33–45, 07 2014.

[3] S. Friedman. Soil properties influencing apparent electrical conductivity: a review. computers and electronics in agriculture, 46: 45-70. *Computers and Electronics in Agriculture*, 46:45–70, 03 2005.

[4] M. A. Hilhorst. A pore water conductivity sensor. *Soil Science Society of America Journal 64 (6), p. 1922-1925*, 64, 11 2000.

[5] P. M. S. Johnson. *The Design of an Integrated Soil Moisture Sensor for Agriculture*. PhD thesis, Griffith University, 2007.

[6] T. Kelleners and A. Verma. Measured and modeled dielectric properties of soils at 50 megahertz. *Soil Science Society of America Journal*, 74:744, 05 2010.

[7] M. A. Malicki and R. T. Walczak. Evaluating soil salinity status from bulk electrical conductivity and permittivity. *European Journal of Soil Science*, 50(3):505–514, 1999.

[8] C. Regalado, A. Ritter, and R. Rodríguez-González. Performance of the commercial wet capacitance sensor as compared with time domain reflectometry in volcanic soils. *Vadose Zone Journal - VADOSE ZONE J*, 6, 08 2007.

[9] J. Rhoades. Electrical conductivity methods for measuring and mapping soil salinity. *Advances in Agronomy*, 49, 12 1993.

[10] A. K. Rêgo Segundo, J. Martins, P. Monteiro, R. Oliveira, and G. Freitas. A novel low-cost instrumentation system for measuring the water content and apparent electrical conductivity of soils. *Sensors*, 15:25546–25563, 10 2015.

[11] F. Visconti and J. M. de Paz. Electrical conductivity measurements in agriculture: The assessment of soil salinity. In L. Cocco, editor, *New Trends and Developments in Metrology*, chapter 5. IntechOpen, Rijeka, 2016.

[12] A. Wilczek, A. Szypłowska, W. Skierucha, J. Ia, V. Pichler, and G. Janik. Determination of soil pore water salinity using an fdr sensor working at various frequencies up to 500 mhz. *Sensors (Basel, Switzerland)*, 12:10890–10905, 12 2012.